Published in final edited form as:
Acta Biomater. 2014 January ; 10(1): . doi:10.1016/j.actbio.2013.10.010.

Multifunctional role of osteopontin in directing intrafibrillar mineralization of collagen and activation of osteoclasts

Douglas E. Rodriguez[1], **Taili Thula-Mata**[1], **Edgardo J. Toro**[2], **Ya-Wen Yeh**[3], **Carl Holt**[4], **L. Shannon Holliday**[2], and **Laurie B. Gower**[1,*]

[1]Department of Materials Science & Engineering, University of Florida, Gainesville, FL, 32611-6400. USA

[2]Department of Orthodontics, University of Florida College of Dentistry, Gainesville, FL, 32610-0444

[3]Department of Biomedical Engineering, University of Florida, Gainesville, FL, 32611-6131

[4]School of Life Sciences, University of Glasgow, Glasgow, G12 8QQ, UK

Abstract

Mineralized collagen composites are of interest because they have the potential to provide a bone-like scaffold that stimulates the natural processes of resorption and remodeling. Working toward this goal, our group has previously shown that the nanostructure of bone can be reproduced using a polymer-induced liquid-precursor (PILP) process, which enables intrafibrillar mineralization of collagen with hydroxyapatite (HA) to be achieved. This prior work used polyaspartic acid (pASP), a simple mimic for acidic non-collagenous proteins (NCPs), to generate nanodroplets/nanoparticles of an amorphous mineral precursor which can infiltrate the interstices of type-I collagen fibrils. In this study we show that osteopontin (OPN) can similarly serve as a process-directing agent for the intrafibrillar mineralization of collagen, even though OPN is generally considered a mineralization inhibitor. We also found that inclusion of OPN in the mineralization process promotes the interaction of mouse marrow-derived osteoclasts with PILP-remineralized bone that was previously demineralized, as measured by actin ring formation. While osteoclast activation occurred when pASP was used as the process-directing agent, using OPN resulted in a dramatic effect on osteoclast activation, presumably because of the inherent arginine-glycine-aspartate acid (RGD) ligands of OPN. By capitalizing on the multifunctionality of OPN, these studies may lead the way to producing biomimetic bone substitutes with the capability of tailorable bioresorption rates.

Keywords

Biomimetic material; biomineralization; bioresorption; bone graft; osteopontin; osteoclast

*Contact Author: Laurie Gower, lgowe@mse.ufl.edu.

1. Introduction

Many researchers are investigating biodegradable polymeric and composite-based biomaterials for potential use as bone grafts, where these synthetic materials are resorbed either through hydrolytic or enzymatic mechanisms. Alternatively, designing biomaterials using a biomimetic approach increases the potential for resorption through osteoclastic resorption; that is, the natural process by which bone is removed by osteoclast cells during remodeling. In this case, the entire bone does not degrade, but instead small canals are resorbed through the bone by osteoclasts, followed closely by osteoblasts that deposit new bone; thus the surrounding bone retains its structural and mechanical integrity throughout the remodeling process. Therefore, for the long-term goal of preparing a bioresorbable load-bearing bone substitute, it could be advantageous for the material to have a more bone-like resorption response that parallels the natural remodeling process. Our approach towards this goal is to emulate the natural processes involved in bone formation in order to develop nano-structured hydroxyapatite (HA)/collagen composites with a bone-like architecture that can serve as such bioresorbable materials.

In our previous work, we have used the polymer-induced liquid-precursor (PILP) mineralization process to generate intrafibrillar mineralization of collagen. In this process, negatively charged acidic polymers (considered simple mimics to the non-collagenous proteins, or NCPs, associated with bone) are added to supersaturated salt solutions in order to sequester ions or clusters that phase separate into droplets of an amorphous mineral precursor that can infiltrate the interstices of the collagen fibrils, leading to a high degree of intrafibrillar mineralization. In contrast, the conventional mineralization reaction without polymer results in heterogeneous nucleation of spherulitic clusters of HA on the surface of the collagen [1-10]. The HA crystals which form within the interior of the collagen fibrils in the PILP process are even oriented in the same way as they are in biogenic bone, aligned with their [001] direction parallel to the long axis of the collagen fibril, which is apparently dictated by the collagen itself [2, 11-13]. This creates an interpenetrating nanostructure which closely resembles that of bone. Using this process, we have been able to mineralize a variety of collagen based scaffolds, including reconstituted type I collagen films prepared in-house [10], or commercially prepared porous collagen scaffolds [2, 9], bovine and turkey tendon [7], demineralized manatee [8] and bovine bone [14], as well are artificial dentin lesions [15]. With the proper reaction conditions, a high degree of mineralization can be achieved, with compositions matching bone (60 - 70 wt% mineral). Lausch et al. have shown this process can be used to remineralize the collagen tissues connecting bones to teeth, and with spatial control apparently dictated by other components retained in the native tissues [13].

Our attention here now turns to whether or not a real non-collagenous protein, such as OPN, can yield mineralization results similar to those achieved with polyaspartic acid (pASP). If OPN can also induce a PILP type mineralization, it would support our hypothesis that this may be one important role of the NCPs in bone mineralization. Given that OPN has a domain with 8 to 10 consecutive aspartic acid residues, along with many phosphorylated residues [16], and the acidic NCPs (such as OPN and Bone sialoprotein) tend to have a flexible and intrinsically disordered structures (non-globular, without well-defined tertiary structure) [17-20], it might be reasonable to expect similar ion interactions with these polyanionic NCPs as seen with pASP. Furthering this possibility, other work has shown OPN to form an amorphous hydrated calcium phosphate / phosphopeptide complex in supersaturated solutions [21], which might be analogous to the PILP phase. This work showed that the calcium phosphate (CaP) nanoclusters are comprised of a spherical core of an amorphous hydrated CaP surrounded by a dense shell of sequestering phosphopeptide [21].

In addition to the putative role these NCPs play in the bone mineralization process, they can also contribute to the mechanical properties [22-25], as well as cell signaling. Thus, if a PILP type mineralization of collagen can be directed by OPN, the OPN will become incorporated throughout the biomimetic bone substitute material, potentially providing biomechanical linkages as well as cell attachment sites. Osteopontin is known to contain RGD-sequences that serve as integrin ligands, and integrin signaling is vital for both osteoclasts bone resorption and osteoblasts function.

From the biomaterials perspective, where such biomimetic HA/collagen composites might be used as bone grafts, we are interested in determining if their bone-like nanostructure might allow for osteoclast resorption for a natural remodeling process. Kikuchi *et al*. [26] have shown that nanostructured collagen-hydroxyapatite composites (prepared by a non-biomimetic method) can be resorbed by phagocytosis by osteoclast-like cells, so it was anticipated that our biomimetic nanostructured composites should also be amenable to osteoclast resorption.

Here, we report on two sets of experiments with the goals to 1) determine if OPN can act as a process-directing agent to generate intrafibrillar mineralization of type-1 collagen scaffolds; and 2) determine if incorporation of OPN into bone-like collagen scaffolds influences osteoclast activation. For the second study, dense bone slices were demineralized and then remineralized back with an OPN-mediated PILP process in order to prepare dense solid substrates that allow osteoclasts to form a sealing zone, which can be readily tracked with a fluorescent marker for determining if they have become activated. These studies demonstrate that OPN can act as a PILP process-directing agent, and that incorporation of the OPN into the matrix promotes osteoclast activation, in contrast to a matrix mineralized by conventional mineralization processes. This may represent a step toward the goal of the construction of fully biocompatible and bioresorbable load-bearing bone substitutes.

2. Materials and Methods

2.1 Bovine OPN Purification

Three hundred milligrams of a bovine milk-derived calcium salt osteopontin mix was purified from bovine milk as previously described [21, 27]. To remove the calcium salt, the peptide mixture was dissolved in 5 ml deionized (DI) water and placed in a dialysis tube with a porosity of 10,000 molecular weight cut-off. The osteopontin solution was dialyzed against 1 L of 1 mM Na_2H_2EDTA and 1.5 mM NaN3 (sodium azide) at 4°C for 1 day. The EDTA solution was then replaced by 1 L of DI water and dialysis was continued for 8 hours at 4°C (3×). The remaining osteopontin was then collected, freeze-dried and stored at −20°C until use. As described in detail elsewhere [21], the final mixture of peptides isolated contains 10 wt% intact OPN (33.9 kDa) and 57 wt% OPN with a molecular weight of 19.8 kDa, attributed to extensive degradation by the main milk proteinase plasmin. The remainder consists of smaller peptides.

2.2 Mineralization of Collagen Sponge

Commercially available collagen sponges (Ace Surgical Supply, Inc.) composed of reconstituted bovine type-I collagen were used as substrates for the mineralization experiments. The mineralization solution was prepared by mixing equal volumes of 9 mM $CaCl_2{\cdot}2H_2O$ (Sigma, St. Louis, MO) and 4.2 mM K2HPO4 (Sigma, St. Louis, MO) solutions, chosen based on the results of our prior studies. To maintain the pH of the mineralization solution at 7.4, calcium and phosphate solutions were made in Tris-buffered saline (TBS) containing 0.9% (w/v) NaCl and 0.02% (w/v) sodium azide (Sigma, St. Louis, MO). OPN-mix was added at a concentration of 200-μg/ml to 20 ml of calcium solution

before mixing an equal volume of the phosphate counterion solution. An additional control group was made where the mineralization solution contained no polymeric additive. The sponges were incubated in the mineralization solution under vacuum conditions for 30 minutes to remove any air bubbles trapped within the porous matrix. After degassing the sample, the mineralization reaction was kept in a 37°C oven to emulate physiological conditions. At 4 days, the mineralized samples were removed from the solution, copiously washed with DI water, lyophilized and stored at −20°C until use.

2.3 Demineralization/Remineralization of Bone Specimens

Bovine bone slices approximately 100 μm thick were cut from the diaphysis of a bovine femur using a wet saw. Specimens reserved as native bone controls were briefly rinsed with DI water following sectioning. Other specimens were demineralized in a 0.5 M EDTA solution (made in Tris buffered saline (TBS), pH adjusted to 8.0 with NaOH) for 3 days. Specimens were then rinsed in DI water for 24 hours. Upon removal from the rinse, specimens were either immediately remineralized or lyophilized and stored at −20 °C.

Demineralized bone specimens were remineralized with calcium phosphate solutions to form HA as described above. Three groups of remineralized samples were made, differentiated by the type of negatively-charged polymer used in the PILP process: i) no polymer additive (conventional remineralization), ii) polyaspartic acid-sodium salt: M_w of 27 kDa (Alamanda Polymers) at a concentration of 100 μg/mL, and iii) osteopontin at a concentration of 100 μg/mL.

2.5 Wide Angle X-Ray Diffraction Analysis

Wide Angle X-Ray Diffraction (WAXD) was performed on unmineralized and mineralized collagen scaffolds as well as on dehydrated native, demineralized, and remineralized bone specimens to assess the phase of calcium phosphate present. A Philips XRD ADP 3720 diffractometer (40 kV, 20 mA) was used in this analysis, using a step size of 0.02° mrad/s with a time per step of 0.5 s and a scan range 2θ of 10°-70°.

2.6.Preparation of Osteoclasts and Osteoclast Activation Assay

Osteoclasts were differentiated from bone marrow cells harvested from Swiss-Webster mice (8-20 g). Mice were sacrificed via cervical dislocation after which femora and tibiae were aseptically dissected from adherent tissue. Proximal and distal ends of the bones were removed and the marrow flushed from the intramedullary canal with αMEM media (10% fetal bovine serum) using a 25 gauge needle. The marrow was rinsed twice with αMEM-10% FBS and plated in 24-well culture dishes at a density of 10^6 nucleated cells/cm^2 with 1 mL of αMEM-10% FBS per well. The culture media was also supplemented with 10 nM 1,25-dihydroxyvitamin D3 (1,25 D3, Invitrogen). The cells were incubated at 37 °C in a humid environment of 5% CO^2 in air for 5 days. At day 3, half of the supplemented media was exchanged. All procedures were approved by the University of Florida Animal Care and Usage Committee.

Using a previously developed method [28], the murine osteoclasts were scraped from the culture dishes after 5 days of culture and plated on the various bone specimens in triplicate in 24- well culture dishes. The cells were plated at a density of 1×10^6 nucleated cells/cm^2 in 1 mL of aMEM (10% FBS, 10 nM 1,25 D3) per well. After incubation for 48 hours, the cells were fixed with 2% formaldehyde in PBS for 20 min, permeabilized with 1% Triton X-100 for 10 min and rinsed with PBS. The cells/specimens were then incubated in 5 μg/mL Texas Red-tagged phalloidin (Sigma Aldrich) for 10 minutes in PBS plus fetal bovine serum to detect actin rings. The antibody used to stain the ruffled membrane green targets the E subunit of vacuolar H^+-ATPase (V-ATPase) enzyme, and was made in the lab, as described

previously [29]. It was detected using FITC-tagged secondary antibody, using the polyclonal anti E subunit antibody at a 1:500 dilution and the second antibody also diluted 1:500.

2.8 Scanning Electron Microscopy

Surfaces of scaffold and bone specimens were examined with scanning electron microscopy (SEM) both pre- and post-culture. Specimens reserved for SEM examination pre-culture were lyophilized after the mineralization procedure, attached to aluminum stubs with double-sided copper tape, and subsequently sputter-coated with carbon. For the specimens examined post-culture, cells were gently scraped off the surface, the specimens rinsed and then dehydrated via graded ethanol baths. These specimens were then mounted on stubs as previously described. A JEOL 6400 SEM instrument (operated at 15 kV) equipped with an attached energy dispersive spectrometer (EDS) was used to take high magnification images.

3. Results

3.1 Mineralization of Collagen Sponges using OPN-mix as Process-Directing Agent

The OPN phosphopeptide mixture, hereafter referred to as OPN-mix, was found to be very effective at mineralizing the collagen sponges, as shown in Figures 1 and 2. As can be seen in the SEM micrographs in Figure 1, the collagen sponge, prior to mineralization, consists of loosely packed fibrils that are relatively smooth in appearance (Fig. 1A). When the sponge is mineralized via the conventional solution crystallization process (without polymer additive), it simply leads to spherulitic clusters of hydroxyapatite on the surface of the substrate (Fig. 1B). The collagen fibrils are not readily discerned in this micrograph because they tend to collapse into a smooth mat upon drying, possibly because of the lack of fixation prior to dehydration. In contrast, when the collagen sponge is mineralized in the presence of OPN-mix to induce the PILP process (Fig. 1C), the fibrils become infiltrated with mineral and do not collapse, thereby highlighting the fibrillar texture. Notably, there are no spherulitic mineral clusters on the surface, but EDS is useful for verifying that mineral is present (Fig. 1D). However, this is also evident from the appearance of the mineralized fibrils, which typically are brighter and exhibit a rougher texture, and there are often lumps and bulges where the mineral has unevenly infiltrated the fibrils. Because the fibrils are being examined in SEM, they are dried under vacuum; therefore, the regions where water was displaced by mineral remain extended upon drying, while any regions that are not filled with mineral collapse upon drying, leading to bulges. The fibrils throughout the scaffold seemed well extended, suggesting that they contain a high degree of mineral. The TEM micrographs in Figures 1E and 1F confirm the presence of intrafibrillar mineral, where the selected area electron diffraction (SAED) pattern is that of HA crystals aligned with the [001] direction oriented parallel to the long axis of the fibril (inset in Fig. 1F). The high degree of mineral content was further verified by X-ray diffraction (XRD) and thermogravimetric analysis (TGA), as shown in Figure 2. The broad XRD peaks are expected for mineral that is composed of small crystallites (Fig. 2A), which is typical of what we have observed in our other studies of intrafibrillar mineral (using pASP) [2, 6-9], and is also the case for bone [30]. The TGA curves show that in fact the fibrils are very well mineralized, containing 75 wt% mineral (Fig. 2B- top curve). The differential thermal analysis (DTA) curve shows a peak at 330 °C (Fig. 2B- bottom curve). Collagen that is well mineralized displays such a low temperature peak [6], as does bone and dentin [31, 32], while pure collagen without mineral exhibits a high temperature peak at around 500 °C [31]. According to the literature, exothermic peaks in the range of 260–360 °C correspond to collagen decomposition, while exothermic peaks in the range of 450–550 °C correspond to collagen combustion. Our prior work shows that the high temperature peak is reduced in the presence of intrafibrillar mineral [8, 9], similarly to that seen in bone and dentin, which suggests that the intimate association between mineral and collagen alters the decomposition products formed at the

first transition to no longer contain thermally stable compounds (presumably doubly- or triply-bonded compounds).

3.2 Demineralization and Remineralization of Bone

Bovine femur bone slices were demineralized through EDTA treatment, which has been shown to retain the supramolecular arrangement of the collagen structure [33]. We then remineralized the bone slices for 7 days using either pASP or OPN-mix as a process-directing agent for comparison. After bone specimens were demineralized and then remineralized, a few specimens from each group were reserved for SEM/EDS analysis. Representative SEM micrographs are shown in Figure 3 along with their respective EDS spectra. The micrograph of the native bone specimen presented in Figure 3A reveals the underlying structure of the plexiform portion of the bovine bone (fibrolamellar units). A typical micrograph of the demineralized bone is shown in Figure 3B. Here it is seen that the underlying collagen organization of the bone is left intact, where the osteons, Haversian canals, and lacunae are clearly seen. In addition, the EDS spectra for the demineralized specimens confirm that there is no calcium and phosphorous present near the surface.

Micrographs of remineralized bone specimens using the PILP process induced with PASP or OPN-mix are presented in Figures 3C and 3D, respectively. The same structure seen in the native bone specimens is observed in these samples as well. The corresponding EDS spectra show the presence of calcium and phosphorous in these specimens, indicating the presence of calcium phosphate. This mineral is assumed to be predominantly intrafibrillar since the SEM images do not show extrafibrillar mineral clusters. The surface appears more rough, however, in the OPN-mix PILP-remineralized sample (Fig. 3D).

For comparison, Figures 4A-4E shows SEM/EDS analysis of demineralized bone remineralized by the conventional crystallization process (no polymer additive). Here it can be seen that it formed a thick mineral crust over the majority of the substrate (Fig. 4A) with interdispersed regions where this crust is not present (Fig. 4B). At higher magnification of the mineral crust (Fig. 4C), one can see the platy structure of the HA crystals, which is typical of HA grown by the conventional crystallization process. This clearly leads to a very different topology that could influence osteoclast interactions.

WAXD spectra of samples from each group are shown in Figure 5. Here the typical peaks for HA at 26° and 32° are confirmed for the native bone sample. As expected, the demineralized sample does not have these peaks related to HA, reinforcing the EDS spectra in demonstrating no presence of the mineral component. These peaks at 26° and 32° begin to show in the PILP- pASP sample whereas they are more prominent in the PILP sample mineralized with OPN-mix acting as the process-directing agent. This enhanced signal may be due to a small amount of mineral build-up on the surface, as seen by the roughness in Figure 3D. Interestingly, the OPN-mix remineralized bone shows a strong peak at 26°, which is barely visible in the XRD of the mineralized sponge (Fig. 2A), even though the sponge was highly mineralized. This may be due to preferential orientation of those planes in the bone specimen since it has a more directionally aligned collagen than the random network of the sponge.

When porous collagen substrates are mineralized with the PILP process, it is visually obvious when the collagen fibrils have become mineralized because they get thicker and sometimes exhibit a rough surface texture from a thin coating of mineral, but with no evidence of surface-bound spherulitic clusters. It is less clear when working with demineralized bone scaffolds because the collagen is so densely packed. The EDS and XRD indicate the presence of a large amount of mineral, and yet very little mineral is seen on the surface of the fibrils because it is predominantly intrafibrillar. Although not studied here, we

expect that the intrafibrillar mineral was [001] oriented, as was demonstrated by TEM in our prior report where we remineralized manatee bone using similar conditions [8].

3.3 Osteoclast Activation

During the natural processes of osteoclastic resorption, the osteoclast adheres to the bone surface and becomes polarized, forming a sealing zone (SZ), which is a ring of very tight adhesion between the osteoclasts and the bone, which segregates an extracellular resorption pit for containment of the harsh components secreted during the resorption process. The actin ring is a microfilament-based structure composed of interconnected, dynamic units called podosomes which are associated with the sealing zone. Bounded by the actin ring is a specialized subdomain of the plasma membrane, the ruffled membrane or ruffled border, which is rich in V-ATPase and facilitates bone degradation by pumping protons and secreting proteases into the resorption compartment [34, 35]. Both of these can be monitored *in situ* using fluorescent staining to determine if osteoclasts have become activated. Their activity can be further verified by the presence of resorption pits which have a morphological appearance that can be readily identified in scanning electron microscopy (SEM).

Osteoclasts derived from murine bone marrow were cultured on native bone, demineralized bone, and remineralized bone samples for 48-hours. Actin rings and ruffled borders were observed on the control native bone samples as shown in Figure 6A and 6B. Very few actin rings and ruffled borders were observed on the surfaces of the demineralized bone, with one small one being seen in Figures 6C and 6D. The conventionally remineralized samples (remineralized without polymer additive) also had relatively few actin rings, but they were a little larger than the demineralized sample, as shown in Figure 6E and 6F. Stress-actin is also observed in these samples whereas none is observed in the bone control group. When looking at the PILP-remineralized samples using pASP, both actin rings and ruffled borders were observed on the surfaces (Figure 6G and H), although the rings were fewer and smaller than those of the positive bone control.

A second independent osteoclast culture was conducted with a control native bone group and a group of PILP-remineralized samples using OPN-mix as the process-directing agent for mineralization. Here it is observed that the PILP-remineralized samples had many more actin rings present when compared to the native bone control (Fig. 7). The diameters of the actin rings on the PILP samples also are similar in scale to those on the bone control samples. Because of the improved activation response in this second cell experiment, a third independent osteoclast culture was conducted testing only the native bone control and PILP-remineralized OPN-mix samples again. Although there were fewer actin rings on the OPN-mix samples in the third cell culture (closer to the number found in the control bone group), the size of the actin rings on the PILP OPN-mix samples were similar. It should be noted that efforts to stain ruffled membranes in this set of experiments was unsuccessful. Unfortunately, staining osteoclasts with anti-E subunit antibodies is an unreliable process due to masking of the antigenic determinant by the complex packing of the 14 different subunits into the V-ATPase enzyme. This was the case for both the OPN-PILP sample and the native bone. Nevertheless, the presence of resorption pits (as detailed in the next section) strongly suggests that ruffled membranes were present.

The total number of activated osteoclasts per specimen for all groups was assessed by the number of actin rings identified, as presented in Figure 8. In the first cell culture study the demineralized and conventionally remineralized samples, and samples remineralized with pASP all have significantly fewer activated osteoclasts compared to the control ($P < 0.01$). Additionally, there was no significant difference of activated osteoclasts between the three treatment groups. In testing the cell response of OPN-remineralized specimens, , the OPN-

mix group had significantly greater the number of activated osteoclasts than the respective control group ($P < 0.001$), with nearly four times the value. In a repeated experiment with the OPN-remineralized specimens, the osteoclast activation was similar between the bone control and remineralized samples with no significant difference between the two groups.

3.4 Presence of Resorption Pits

To determine if the activated osteoclasts are actually able to resorb these bone-like matrices, SEM examinations of post-culture specimens of PILP-OPN-mix were conducted (Fig. 9). Representative resorption pits in the control (native bone) samples are shown in Figures 9A and 9B. Here the pits are clearly seen and have sharp boundaries between resorbed and unresorbed areas. It is also observed that the resorption pits typically occur in clusters of multiple pits grouped together.

SEM micrographs of PILP-OPN-mix samples are shown in Figures 9C-9F. In Figures 9C and 9D, typical resorption pits, identified by black arrows, are not quite as obvious as those seen in the control samples. When compared to SEM micrographs of the surface pre-culture (Figure 3D), however, it is obvious that the regions of interest are not a result of the surface appearance of the specimens, but rather are attributed to the resorptive behavior of the osteoclasts. Most of the pits observed do not have a sharp-edged boundary except in a few cases. Higher magnification images of Figures 9C and 9D are shown in Figures 9E and 9F, respectively, which shows examples of sharp and non-sharp boundaries. This may be due to the rougher surface of the specimens, which seemed to be more prominent for the OPN-mix remineralized specimens. It also appears that the resorption pits are less clustered than those seen in the control samples.

4. Discussion

4.1 Collagen Mineralization with OPN

In this study, we show that intrafibrillar mineralization of collagen can be induced by the most abundant non-collagenous protein in bone, osteopontin (OPN). Intrafibrillar mineralization of collagen has been demonstrated *in vitro* for other NCPs by groups who have examined fetuin [11] and phosphorylated dentin matrix protein-1 (DMP1) and dentin phosphophoryn (DPP) [36]. In the dentin proteins, interesting differences were observed between the amount of intra- versus extra-fibrillar content, as well as crystal alignment. The overall morphology and nanostructure in all of these studies appear very similar to those produced with pASP by our group and others, suggesting that this occurs via infiltration of PILP droplets. Given the similarities in nanostructure to native bone, this further supports our hypothesis that this could be the primary role of some of the acidic non-collagenous proteins associated with bone and dentin. In other words, the acidic proteins may first promote the intrafibrillar mineral by inhibiting classical nucleation in the extrafibrillar space. After intrafibrillar mineral is formed, any remaining OPN could further interact with extrafibrillar crystals to modify their growth habit by the adsorptive mechanisms more commonly discussed. We have always found it interesting that in our in vitro model system, the intrafibrillar space of collagen fibrils becomes mineralized first, which is then followed by an extrafibrillar mineral coating. The cryo-EM images provided by Nudelman et al. [11] also seem to show that intrafibrillar mineral is formed first, which would be somewhat unexpected if the particles/droplets were simply adsorbing due to electrostatic attraction to (+) residues, as they suggest, because the charged residues are presumably on both the interior and surface of the fibrils. Perhaps the adsorption of some of the acidic proteins to the collagen, as has been well documented [37], provides a “protective” coating to keep PILP droplets from adsorbing and coating the collagen with mineral, which could block the entry points (gap zones) for infiltration of PILP droplets. Thus, rather than the traditional

hypothesis which considers adsorption of NCPs to collagen to serve a promotory role on crystal nucleation, it might serve the purpose of enabling droplet entry into gap zones to properly mineralize the fibril from inside-out.

It should be noted, however, that the OPN-mix we used here was extracted from bovine milk [21], and therefore there are some differences between the osteopontin associated with bone, which is not as highly phosphorylated. For example, in rat bone, OPN has 29 potential phosphorylation sites, but only about 13 of these sites are phosphorylated. The average degree of phosphorylation of the 28 potential phosphorylation sites in the whole protein from milk was 79% [21, 27]. However, there are many proteases present in bone, so degree of phosphorylation of OPN during its active state is not really known. In any case, most regions of the protein have conserved sequences, such as the RGD site, a thrombin cleavage site, an acidic domain at the amino terminus containing 8-10 consecutive aspartic acid residues, as well as serine/threonine phosphorylation sites [16]. Given these similarities, milk-derived OPN seems to provide a useful system for modeling the role of NCPs in bone mineralization as well as cell interactions. In addition, it is known that the highly phosphorylated OPN in milk is associated with casein micelles that stabilize amorphous calcium phosphate (ACP) [38]. In its use here, without the casein, it still apparently provides a mode of action of stabilizing the amorphous CaP phase, and quite possibly one that is a fluidic nanodroplet (although that remains to be proven). We speculate that under our mineralizing reaction conditions, which use only micromolar levels of OPN, the CaP nanoclusters are not in the stable regime, as defined by Holt *et al*. [21], and therefore accumulate to form what we have referred to as PILP droplets. In the biological realm, not only will the concentration of protein influence this inhibitory activity, but the processed state of a protein would be expected to have a marked influence on inhibitory activity, both with respect to cleavage into smaller fragments, as well as degree of phosphorylation or glycosylation [39-41]. Indeed, we have found that the molecular weight of the polymer [6, 9], as well as charge density [42-44], can have a pronounced impact on its ability to induce the PILP process and promote intrafibrillar collagen mineralization.

4.2 Osteoclast Interactions with Remineralized Bone Matrix

Aqueous EDTA treatment of bone has been shown to remove non-collagenous proteins from the organic matrix [45, 46], while retaining the supramolecular structure [47], so it is likely that the only components present in the remineralized substrates are collagen, hydroxyapatite, and the negatively-charged polymer used in the mineralization process. Clearly, if there are any remnant NCPs, they are not at sufficient levels to affect the mineralization, or the osteoclast behavior, since the conventional remineralization of the same demineralized bone matrix served as a negative control.

In previous work, it has been suggested that osteoclast contact with the mineral component of bone may serve to induce bone resorption, based on results of non-resorption of demineralized rabbit bone [48], as well as bone which has a layer of organic matrix on the surface [49]. As such, it is not surprising that the demineralized bone specimens in this study showed relatively little osteoclast activation and resorption. When presented with HA mineral in a non-biomimetic bone structure, as in the conventionally remineralized collagen substrates, the osteoclasts here exhibited little more activation than the demineralized specimens, with only a few actin rings present. The osteoclast response to this group could be because of the dissimilar arrangement of HA and collagen compared to that of native bone, which essentially consists of clusters of large platy crystallites coating the surface of the organic matrix (Fig. 4C), so the cells were primarily only in contact with the inorganic coating, creating a scenario similar to previous work performed by others in which osteoclasts were cultured on anorganic bone. In that work, it was found that osteoclasts only

adhered to the anorganic bone if the substrate was first coated with an adherent factor (vitronectin) [50]. Thus, it is not surprising that we did not observe much osteoclast activation in the conventionally remineralized group. Certainly the surface roughness, which is known to affect osteoclast activity [51], could be a factor as well since it is quite pronounced on the mineralized coating. Other groups have examined HA films prepared by a similar conventional crystallization method (*i.e*., they formed a dense mineral crust of platy HA crystals), and in those cases did see osteoclast resorption, as measured by pits in the calcium phosphate coated plastic substrates [52, 53]. These studies utilized a different system to produce osteoclasts. In our hands, calcitriol-stimulated mouse marrow cultures failed to resorb similar calcium phosphate-coated substrates (L. Shannon Holliday and Stephen L. Gluck, unpublished results).

In contrast, the PILP-remineralize bone specimens did show more osteoclast interactions. They were relatively modest (lower than the positive bone control) when pASP was used for the mineralization; nevertheless, it does appear that by reconstituting a more native bone nanostructure, it helped to restore some type of osteoclast interactions. Presumably having the smaller HA crystals which are intimately associated with the collagen somehow became more recognizable by the cells. Taking this a step further, when the PILP remineralization was performed with the OPN-mix, the osteoclast interactions were dramatically improved, even above and beyond the positive bone control (in one trial). This can most likely be attributed to the RGD ligand that is present on the OPN, which can then interact through the αvβ3-integrin (vitronectin receptor) of osteoclasts [54-56]. Indeed, Reinholt *et al*. found OPN and vitronectin receptors to be co-localized at regions where osteoclasts attached to the bone surface (clear zone), supporting their hypothesis that OPN serves as an anchor binding the bone mineral to the vitronectin receptors identified on the osteoclast plasma membrane [57]. McKee and coworkers have also shown that OPN is accumulated in lamina limitans and is involved with osteoclast adhesion [58-60]. Addison et al. and McKee et al. have proposed that there are atomic-level electrostatic mechanisms of OPN peptide binding to crystal surfaces [61, 62]. Nakamura et al. [54] studies on αvβ3-integrin show that it plays a role in the regulation of two processes required for effective osteoclastic bone resorption: cell migration and maintenance of the sealing zone. In our *in vitro* system, apparently not all of the OPN is absorbed into the substrates and some is present at the surface. Because this did not occur for the negative control (mineralized with conventional crystallization), this seems to confirm that the EDTA treatment did effectively remove most non-collagenous proteins, which presumably could have led to some osteoclast interactions if present. One might ask why the RGD domains in collagen itself did not trigger this enhanced osteoclast activity? Apparently, it requires cleavage or denaturation of the collagen in order to expose the cryptic RGD-sequences that initiate osteoclast bone resorption [56]. This can occur through interstitial collagenase, which is produced by osteoblasts, acting as a “coupling factor” that allows osteoblasts to initiate bone resorption by generating collagen fragments that activate osteoclasts [63].

Further studies are needed to more closely examine the osteoclast behavior, to determine if there is a reason the resorption pits look a little different for the remineralized bone specimens. This could be simply related to the surface roughness [51, 64], or even subtle changes in the podosome or ruffled border activities. Even the spatial organization of the adhesive ligands can play a role, which in our *in vitro* system, is not regulated. For example, Anderegg *et al*. [65] used micro-patterned surfaces, consisting of adhesive domains of vitronectin separated by non-adhesive domains, and found that the sealing zone expansion is dependent on the continuity of matrix adhesiveness. Other studies have indicated that the overall size and dynamics of sealing zones depend on the chemical and physical properties of the underlying substrate [51, 64, 66, 67]. For example, on bone, SZs are rather small and relatively stable (and there can be more than one per cell), whereas on vitronectin-coated

glass surfaces, the SZs fuse into one large ring, and are highly dynamic and apparently unstable [65, 66].

There was considerable variability between the osteoclast cultures on the two groups of OPN-mineralized specimens, the reason for which remains to be determined, but is perhaps related to surface roughness (see Figs. 9A-F), which has been shown to influence osteoclast activity [68, 69] [50, 51]. Whether this is the primary cause of the variability cannot be determined from this study, but this does not take away from the results that both independent cultures with OPN-mineralized substrates exhibited strong interactions with the osteoclasts. This is an exciting result because it suggests that one might actually be able to tailor the rate of resorption in a bone graft material simply by adjusting the level of osteoclast interactions through their interactions with the additives. For example, variable levels of pASP with OPN could be used, or it might even be as simple as adding in RGD sequences to the additive. Indeed, in native bone, the expression of osteopontin mRNA is especially high at sites destined for resorption [70], which may be desirable for a bioresorbable bone substitute.

4.3 Proposed Role of OPN In Bone Mineralization

In recent years it has been shown that many of the acidic proteins associated with biominerals fall in the class of intrinsically disordered proteins (IDPs), including OPN [71], bone sialoprotein, and phosphophoryn [18, 71]. Therefore, new hypotheses have arisen suggesting that the flexibility of the proteins can assist with interactions between multiple ions in the mineral crystal faces [71], and that this can occur through more general electrostatic interactions [72], as opposed to the prior view that these NCPs had very specific conformations that led to epitaxial-like relationships with the mineral [73]. Our view differs from these hypotheses in that we believe a primary role of these flexible proteins is to interact with the ionic species and/or clusters (not crystal faces), to sequester them into fluidic mineral precursor droplets that can infiltrate collagen fibrils via capillary action [2]. While it is certainly possible that these anionic proteins can interact with crystal faces, which could be a means for modulating crystal size, shape and orientation [36], this would seemingly be more relevant to the extrafibrillar crystals, because once the mineral precursor is infiltrated inside the collagen fibrils, its crystal properties seem to be directed more by the collagen compartment [2, 11, 74]. It should be noted that our hypothesis does not contradict the many prior studies that have shown that OPN is inhibitory to crystal nucleation and growth. It is precisely this inhibitory activity that keeps the supersaturated solution free of crystalline precipitates, while the polymer/protein is sequestering ions to form PILP droplets, which can then infiltrate the collagen fibrils, and in such a way that the interior fills with mineral precursor first [5, 11]. *In vivo*, such a precursor phase could presumably be formed as the NCPs are secreted by osteoblasts into the ECM. In addition, spatio/temporal control may occur through enzymatic processing of the proteins into their most active form [40]. In the case of dentin, which is also a collagen-based hard tissue, proteins are secreted through dentin tubules, where the highly acidic phosphophoryn protein would be a likely candidate to lead to a similar PILP process.

OPN is often considered an inhibitory protein, but the fact that OPN is intimately associated with the mineral phase in bone [75] and in osteoblast cultures [76], as shown by immunocytochemical labeling, is seemingly not consistent with that perspective. Indeed, OPN and osteocalcin genes are expressed at or near the time of mineralization [77], which would seem more consistent with our hypothesis that they are there to promote intrafibrillar mineralization of the collagen matrix (where inhibition of the conventional crystallization reaction leads to a PILP type reaction). On the other hand, OPN-deficient mice do not show any macroscopic structural alterations in bones at birth and during further development [78].

At the microscale, FTIR microspectroscopy of OPN-deficient mice revealed that the relative amount of mineral in the more mature regions of the bone (central cortical bone) was significantly increased, and the mineral crystal size and perfection was increased throughout all the bone [79]. The authors attributed these changes to either OPN-inhibition of mineral crystal growth or to potential effects of OPN on bone cell response. Our *in vitro* results seem to support the latter scenario, where the lack of OPN would be expected to reduce interactions with osteoclasts and thus bone turnover and remodeling, which in turn would lead to more mature crystallites over time (as well as more mature collagen, which was also measured in their studies). Indeed, it has been found that bone resorption is decreased in OPN-deficient mice relative to wild-type where both are given a Ca-deficient diet [80]. Additional support for the altered osteoclast function in OPN-deficient mice is provided by Franzén *et al*. [81], who have shown in OPN knockout mice that the volume and length of the osteoclast ruffled border was several folds lower, indicating a lower resorptive capacity.

Returning to the fact that OPN-deficient mice are still able to mineralize bone without using OPN seems to indicate that there are other NCPs which must also play a role of promoting collagen mineralization. Combinations of the NCPs may be used to more precisely regulate the overall mineral structure, as well as cell signaling functions, which in the case of OPN, would seemingly be involved in regulating the osteoclast pathway for bone resorption. OPN has also been considered an “inhibitory” protein in bone mineralization because it reduces the formation of mineral nodules in osteoblast cell cultures, and is a negative regulator of proliferation and differentiation in MC3T3-E1 cells [82] (although there seem to be contradictory findings in the literature, depending on the exact experimental system used [83-87]). This type of inhibitory activity could also be from cell signaling effects. It certainly makes sense that as osteoblasts encounter bone matrix that has already been mineralized, that the remnants of the mineralization, such as OPN, would signal to the cells to stop making bone in that location. Perhaps this is why OPN is a late marker of bone mineralization, while other NCPs (such as BSP) may be involved in the earlier stages of mineralization [88]. In other words, the NCPs may be redundant in terms of helping to promote the proper kind of collagen mineralization (which does not require a high degree of protein structure or specificity when using the PILP process), but the temporal sequences of addition of the NCPs may be related to their specific cell signaling functions, which might be expected to change as the matrix is just starting to mineralize versus when the mineralization is nearly complete.

We are proposing here that the biological function of non-collagenous proteins found in bone, such as OPN, is to promote mineralization in bone formation, albeit via a very specific type of mineralization. But this leads to the question- why are the same types of proteins located in places where the normal physiological function would seemingly need to inhibit mineralization? For example, OPN and matrix Gla protein are found in calcified vasculature [89, 90], and OPN is intimately associated with kidney stones [91-95]. A potential resolution to this apparent paradox can be found in the work of Holt *et al*. [21], who found that in a supersaturated solution containing a certain concentration of competent sequestering phosphoprotein, ions are initially sequestered in the form of stable nanoclusters by a stoichiometric excess of the phosphoprotein. But as ions continue to accumulate and eventually form a stoichiometric excess over the phosphoprotein, the surplus of ions grow into a bulk amorphous phase, which ultimately will transform into a crystalline phase. Extrapolating these *in vitro* observations to *in vivo* situations, one could see that if the inhibitory activity of OPN is overcome by excess ions, this could lead to collagen mineralization in bones and teeth, as well as the unfortunate consequence of pathological deposits. In the opposite scenario, if there was a surplus of phosphoprotein, as found in accumulation of excess OPN in the X-linked hypophosphatemia, the ions may be overly stabilized and could potentially lead to decreased bone mineralization, which has been

observed as osteoidosis in mouse models [40]. It is interesting to note that Beck *et al*. [77] find that OPN is induced in direct response to increased phosphate levels, which could provide a mechanism to explain how expression of OPN is normally regulated in bone, where it may become up-regulated to provide a signature to the final stages of mineralization. It also suggests how it may become up-regulated in response to pathological deposits, where its function may be intended to be inhibitory, yet it could simply become overwhelmed with a stoichiometric excess of ions over the phosphoprotein. This can lead to interesting consequences, as we discuss in our papers considering the relevance of PILP to kidney stones [96-98].

5.Conclusions

Preliminary studies were done using a commercially available collagen sponge to determine if osteopontin could be used to induce the PILP process and direct intrafibrillar mineralization of type-I collagen. Indeed, TGA showed that 75 wt% mineral could be attained using OPN as a process-directing agent, and most of the mineral appeared to be intrafibrillar, as evidenced by TEM and the fact that large calcium and phosphorous EDS peaks are present even though external mineral is not observed. These results demonstrate that proteins that are inhibitory to crystal nucleation and growth, due to their ion-sequestering activity, can lead to an alternative pathway of mineralization that actually assists in the intrafibrillar mineralization of collagen scaffolds, thereby offering a plausible explanation for their involvement in both bone mineralization and prevention of pathological mineralization.

Our *in vitro* model system suggests that OPN has a multifunctional role with respect to modulating both the mineralization reaction, as well as the cellular activity. Thus, it becomes quite complex when trying to unravel its role *in vivo*. Simply considering a protein to be “inhibitory” is not the end of the story, where it is clear that this inhibitory activity can promote the intrafibrillar mineralization of collagen. In contrast, OPN's modulation of cellular activities could also alter the mineral content in bone, where this type of “inhibitory” activity could relate to osteoblast or osteoclast activities, with the latter being particularly important in bone remodeling. Thus, the second part of the study took advantage of the multifunctionality of OPN and examined osteoclast interactions with PILP-remineralized bone specimens and found that both the bone nanostructure played a role in activating osteoclasts, as well as the organic ligands present in the OPN. These results suggest PILP processing may be able to lead to biomimetic bone graft substitutes that are bioresorbable through the cellular processes of bone remodeling (as opposed to materials based on hydrolytic degradation that require matching to bone in-growth rate), and that the bioresorption rate might be tunable by adjusting the ligands associated with the process-directing agent. When considering the interactions of non-collagenous proteins, serum adhesion proteins, cytokines, hormones, topography, composition, *etc*., it is evident that osteoclastic activation and resorption is a complex mechanism, so our ability to make biomimetic bone with controlled addition of constituents could be a useful model system for further examining these issues.

Acknowledgments

This work was supported by the National Science Foundation (grant No. DMR-0710605), National Institutes of Health (grant No. RO1-DK092311), and UF-HHMI Science for Life Program. Any opinions, findings and conclusions or recommendations expressed in this material are those of the author(s) and do not necessarily reflect those of the National Science Foundation. The authors confirm that there are no known conflicts of interest associated with this publication and there has been no significant financial support for this work that could have influenced its outcome.

References

1. Gower LB. Biomimetic Model Systems for Investigating the Amorphous Precursor Pathway and Its Role in Biomineralization. Chemical Reviews. 2008; 108:4551–627. [PubMed: 19006398]
2. Olszta MJ, Cheng XG, Jee SS, Kumar R, Kim YY, Kaufman MJ, et al. Bone structure and formation: A new perspective. Materials Science & Engineering R-Reports. 2007; 58:77–116.
3. Olszta MJ, Odom DJ, Douglas EP, Gower LB. A new paradigm for biomineral formation: Mineralization via an amorphous liquid-phase precursor. Connective Tissue Research. 2003; 44:326–34. [PubMed: 12952217]
4. Gower LB, Odom DJ. Deposition of calcium carbonate films by a polymer-induced liquid-precursor (PILP) process. J Crystal Growth. 2000; 210(4):719–34.
5. Jee SS, Culver L, Li Y, Douglas EP, Gower LB. Biomimetic mineralization of collagen via an enzyme-aided PILP process. Journal of Crystal Growth. 2010; 312:1249–56.
6. Jee SS, Thula TT, Gower LB. Development of bone-like composites via the polymer-induced liquid-precursor (PILP) process. Part 1: Influence of polymer molecular weight. Acta Biomaterialia. 2010; 6:3676–86. [PubMed: 20359554]
7. Jee SS, Kasinath RK, DiMasi E, Kim YY, Gower L. Oriented hydroxyapatite in turkey tendon mineralized via the polymer-induced liquid-precursor (PILP) process. CrystEngComm. 2011; 13:2077–83.
8. Thula TT, Rodriguez DE, Lee MH, Pendi L, Podschun J, Gower LB. In vitro mineralization of dense collagen substrates: A biomimetic approach toward the development of bone-graft materials. Acta Biomaterialia. 2011; 7(8):3158–69. [PubMed: 21550424]
9. Thula TT, Svedlund F, Rodriguez DE, Podschun J, Pendi L, Gower LB. Mimicking the Nanostructure of Bone: Comparison of Polymeric Process-Directing Agents. Polymers. 2011; 3(1): 10–35. [PubMed: 22328971]
10. Li Y, Thula TT, Jee S, Perkins SL, Aparicio C, Douglas EP, et al. Biomimetic Mineralization of Woven Bone-Like Nanocomposites: Role of Collagen Cross-Links. Biomacromolecules. 2012; 13:49–59. [PubMed: 22133238]
11. Nudelman F, Pieterse K, George A, Bomans PHH, Friedrich H, Brylka LJ, et al. The role of collagen in bone apatite formation in the presence of hydroxyapatite nucleation inhibitors. Nature Materials. 2010; 9:1004–9.
12. Wang Y, Azais T, Robin M, Vallee A, Catania C, Legriel P, et al. The predominant role of collagen in the nucleation, growth, structure and orientation of bone apatite. Nature Materials. 2012; 11:724–33.
13. Lausch AJ, Quan BD, Miklas JW, Sone ED. Extracellular Matrix Control of Collagen Mineralization In Vitro. Advanced Functional Materials. 2013 n/a-n/a.
14. Jee, SS. The Development of Collagen-Hydroxyapatite Nanostructured Composites via a Calcium Phosphate Precursor Mechanism [Dissertation]. Gainesville, FL: University of Florida; 2008.
15. Burwell AK, Thula-Mata T, Gower LB, Habeliz S, Kurylo M, Ho SP, et al. Functional Remineralization of Dentin Lesions Using Polymer-Induced Liquid-Precursor Process. PLoS One. 2012; 7(6):e38852. [PubMed: 22719965]
16. Sodek J, Ganss B, McKee MD. Osteopontin. Critical Reviews in Oral Biology & Medicine. 2000; 11:279–303. [PubMed: 11021631]
17. Fisher LW, Torchia DA, Fohr B, Young MF, Fedarko NS. Flexible Structures of SIBLING Proteins, Bone Sialoprotein, and Osteopontin. Biochemical and Biophysical Research Communications. 2001; 280:460–5. [PubMed: 11162539]
18. Cross KJ, Huq NL, Reynolds EC. Protein dynamics of bovine dentin phosphophoryn. J Pept Res. 2005; 66:59–67. [PubMed: 16000119]
19. Platzer G, Schedlbauer A, Chemelli A, Ozdowy P, Coudevylle N, Auer R, et al. The metastasis-associated extracellular matrix protein osteopontin forms transient structure in ligand interaction sites. Biochemistry. 2011; 50(27):6113–24. [PubMed: 21609000]
20. Gericke A, Qin C, Spevak L, Fujimoto Y, Butler WT, Sorensen ES, et al. Importance of phosphorylation for osteopontin regulation of biomineralization. Calcified Tissue International. 2005; 77:45–54. [PubMed: 16007483]

21. Holt C, Sorensen ES, Clegg RA. Role of calcium phosphate nanoclusters in the control of calcification. FEBS Journal. 2009; 276:2308–23. [PubMed: 19292864]
22. Fantner GE, Hassenkam T, Kindt JH, Weaver JC, Birkedal H, Pechenik L, et al. Sacrificial bonds and hidden length dissipate energy as mineralized fibrils separate during bone fracture. Nature Materials. 2005; 4:612–6.
23. Fantner GE, Adams J, Turner P, Thurner PJ, Fisher LW, Hansma PK. Nanoscale Ion Mediated Networks in Bone: Osteopontin Can Repeatedly Dissipate Large Amounts of Energy. Nano Letters. 2007; 7:2491–8. [PubMed: 17645366]
24. Hansma PK, Fantner GE, Kindt JH, Thurner PJ, Schitter G, Turner PJ, et al. Sacrificial bonds in the interfibrillar matrix of bone. Journal of Musculoskeletal & Neuronal Interactions. 2005; 5:313–5. [PubMed: 16340118]
25. Thurner PJ, Erickson B, Turner P, Jungmann R, Lelujian J, Proctor A, et al. The Effect of NaF In Vitro on the Mechanical and Material Properties of Trabecular and Cortical Bone. Advanced Materials. 2009; 21:451–+.
26. Kikuchi M, Itoh S, Ichinose S, Shinomiya K, Tanaka J. Self-organization mechanism in a bone-like hydroxyapatite/collagen nanocomposite synthesized in vitro and its biological reaction in vivo. Biomaterials. 2001; 22:1705–11. [PubMed: 11396873]
27. Sorensen ES, Hojrup P, Petersen TE. Posttranslational modifications of bovine osteopontin - identification of 28 phosphorylation and 3 o-glycosylation sites. Protein Science. 1995; 4:2040–9. [PubMed: 8535240]
28. Holliday LS, Dean AD, Greenwald JE, Glucks SL. C-type natriuretic peptide increases bone resorption in 1,25-dihydroxyvitamin D3-stimulated mouse bone marrow cultures. JBiolChem. 1995; 270(32):18983–9.
29. Chen SH, Bubb MR, Yarmola EG, Zuo J, Jiang J, Lee BS, et al. Vacuolar H+-ATPase binding to microfilaments: regulation in response to phosphatidylinositol 3-kinase activity and detailed characterization of the actin-binding site in subunit B. JBiolChem. 2004; 279(9):7988–98.
30. Weiner, S.; Traub, W. Organization of Crystals in Bone. In: Suga, S.; Nakahara, H., editors. Mechanisms and Phylogeny of Mineralization in Biological Systems. NY: Springer-Verlag; p. 1991p. 247-53.
31. Lozano LF, Pena-Rico MA, Heredia A, N-Flores JO, Velazquez R, Belio IA, et al. Thermal analysis study of human bone. Journal of Materials Science. 2003; 38:4777–82.
32. Sakae T, Mishima H, Kozawa Y, Legeros RZ. Thermal Stability of Mineralized and Demineralized Dentin: A Differential Scanning Calorimetric Study. Connective Tissue Research. 1995; 33(1-3): 193–6. [PubMed: 7554954]
33. Chen J, Burger C, Krishnan CV, Chu B, Hsiao BS, Glimcher MJ. In vitro mineralization of collagen in demineralized fish bone. Macromolecular Chemistry and Physics. 2005; 206:43–51.
34. Netter, FH. Musculoskeletal system: anatomy, physiology, and metabolic disorders. Summit, New Jersey: Ciba-Geigy Corporation; 1987.
35. Holliday LS, Welgus HG, Hanna J, Lee BS, Lu M, Jeffrey JJ, et al. Interstitial Collagenase Activity Stimulates the Formation of Actin Rings and Ruffled Membranes in Mouse Marrow Osteoclasts. CalcifTissue Int. 2003 Jan 15.
36. Deshpande AS, Fang PA, Zhang X, Jayaraman T, Sfeir C, Beniash E. Primary Structure and Phosphorylation of Dentin Matrix Protein 1 (DMP1) and Dentin Phosphophoryn (DPP) Uniquely Determine Their Role in Biomineralization. Biomacromolecules. 2011; 12:2933–45. [PubMed: 21736373]
37. George A, Veis A. Phosphorylated proteins and control over apatite nucleation, crystal growth, and inhibition. Chemical Reviews. 2008; 108:4670–93. [PubMed: 18831570]
38. Kumura H, Minato N, Shimazaki K-i. Inhibitory activity of bovine milk osteopontin and its fragments on the formation of calcium phosphate precipitates. Journal of Dairy Research. 2006; 73:449–53. [PubMed: 16848930]
39. Boskey AL, Christensen B, Taleb H, Sørensen ES. Post-translational modification of osteopontin: Effects on in vitro hydroxyapatite formation and growth. Biochemical and Biophysical Research Communications. 2012; 419:333–8. [PubMed: 22342723]

40. Barros NMT, Hoac B, Neves RL, Addison WN, Assis DM, Murshed M, et al. Proteolytic processing of osteopontin by PHEX and accumulation of osteopontin fragments in Hyp mouse bone, the murine model of X-linked hypophosphatemia. Journal of Bone and Mineral Research. 2013; 28:688–99. [PubMed: 22991293]
41. Omelon S, Georgiou J, Henneman ZJ, Wise LM, Sukhu B, Hunt T, et al. Control of Vertebrate Skeletal Mineralization by Polyphosphates. PLoS One. 2009; 4
42. Dai, L. Mechanistic Study of the Polymer-Induced Liquid-Precursor (PILP) Process: Relevance to Biomineralization [Dissertation]. Gainesville, FL: University of Florida; 2005.
43. Dai LJ, Cheng XG, Gower LB. Transition Bars during Transformation of an Amorphous Calcium Carbonate Precursor. Chemistry of Materials. 2008; 20:6917–28.
44. Gower, LB.; Anonymous; Olszta, MJ. US 07455854: Method for producing a mineral fiber. University of Florida Research Foundation Inc; 2008.
45. Delmas PD, Tracy RP, Riggs BL, Mann KG. Identification of the noncollagenous proteins of bovine bone by two-dimensional gel-electrophoresis. Calcified Tissue International. 1984; 36(3): 308–16. [PubMed: 6432294]
46. Dickson IR, Jande SS. Effects of demineralization in an ethanolic solution of triethylammonium EDTA on solubility of bone-matrix components and on ultrastructural preservation. Calcified Tissue International. 1980; 32(2):175–9. [PubMed: 6773635]
47. Chen J, Burger C, Krishnan CV, Chu B, Hsiao BS, Glimcher MJ. In Vitro Mineralization of Collagen in Demineralized Fish Bone. Macromolecular Chemistry and Physics. 2005; 206:43–51.
48. Chambers TJ, Thomson BM, Fuller K. Effect of substrate composition on bone-resorption by rabbit osteoclasts. Journal of Cell Science. 1984; 70:61–71. [PubMed: 6501437]
49. Chambers TJ, Fuller K. Bone cells predispose bone surfaces to resorption by exposure of mineral to osteoclastic contact. JCell Sci. 1985; 76:155–65. [PubMed: 4066784]
50. Fuller K, Ross JL, Szewczyk KA, Moss R, Chambers TJ. Bone Is Not Essential for Osteoclast Activation. PLoS One. 2010; 5(9):e12837. [PubMed: 20862258]
51. Geblinger D, Zink C, Spencer ND, Addadi L, Geiger B. Effects of surface microtopography on the assembly of the osteoclast resorption apparatus. Journal of the Royal Society, Interface/the Royal Society. 2012; 9:1599–608.
52. Patntirapong S, Habibovic P, Hauschka PV. Effects of soluble cobalt and cobalt incorporated into calcium phosphate layers on osteoclast differentiation and activation. Biomaterials. 2009; 30:548–55. [PubMed: 18996589]
53. Yang L, Perez-Amodio S, Barrère-de Groot FYF, Everts V, van Blitterswijk CA, Habibovic P. The effects of inorganic additives to calcium phosphate on in vitro behavior of osteoblasts and osteoclasts. Biomaterials. 2010; 31:2976–89. [PubMed: 20122718]
54. Nakamura I, Pilkington MF, Lakkakorpi PT, Lipfert L, Sims SM, Dixon SJ, et al. Role of alpha(v)beta(3) integrin in osteoclast migration and formation of the sealing zone. Journal of Cell Science. 1999; 112:3985–93. [PubMed: 10547359]
55. Duong LT, Lakkakorpi Pi, Nakamura I, Rodan GA. Integrins and signaling in osteoclast function. Matrix Biology. 2000; 19:97–105. [PubMed: 10842093]
56. Duong LT, Rodan GA. Regulation of Osteoclast Formation and Function. Reviews in endocrine & metabolic disorders. 2001; 2:95–104. [PubMed: 11704983]
57. Reinholt FP, Hultenby K, Oldberg A, HeinegÃ¥rd D. Osteopontin--a possible anchor of osteoclasts to bone. Proceedings of the National Academy of Sciences. 1990; 87:4473–5.
58. McKee, MD.; Nanci, A. Osteopontin and the bone remodeling sequence- Colloidal-gold immunocytochemistry of an interfacial extracellular-matrix protein. In: Denhardt, DT.; Butler, WT.; Chambers, AF.; Senger, DR., editors. Osteopontin: Role in Cell Signalling and Adhesion. New York: New York Acad Sciences; 1995. p. 177-89.
59. McKee MD, Nanci A. Secretion of osteopontin by macrophages and its accumulation at tissue surfaces during wound healing in mineralized tissues: A potential requirement for macrophage adhesion and phagocytosis. Anat Rec. 1996; 245:394–409. [PubMed: 8769675]
60. McKee MD, Nanci A. Osteopontin at mineralized tissue interfaces in bone, teeth, and osseointegrated implants: Ultrastructural distribution and implications for mineralized tissue

formation, turnover, and repair. Microscopy Research and Technique. 1996; 33:141–64. [PubMed: 8845514]

61. Addison WN, Nakano Y, Loisel T, Crine P, McKee MD. MEPE-ASARM Peptides Control Extracellular Matrix Mineralization by Binding to Hydroxyapatite: An Inhibition Regulated by PHEX Cleavage of ASARM. Journal of Bone and Mineral Research. 2008; 23:1638–49. [PubMed: 18597632]
62. McKee MD, Nakano Y, Masica DL, Gray JJ, Lemire I, Heft R, et al. Enzyme Replacement Therapy Prevents Dental Defects in a Model of Hypophosphatasia. Journal of Dental Research. 2011; 90:470–6. [PubMed: 21212313]
63. Holliday LS, Welgus HG, Fliszar CJ, Veith GM, Jeffrey JJ, Gluck SL. Initiation of osteoclast bone resorption by interstitial collagenase. J Biol Chem. 1997; 272(35):22053–8. [PubMed: 9268345]
64. Geblinger D, Addadi L, Geiger B. Nano-topography sensing by osteoclasts. Journal of Cell Science. 2010; 123:1503–10. [PubMed: 20375065]
65. Anderegg F, Geblinger D, Horvath P, Charnley M, Textor M, Addadi L, et al. Substrate Adhesion Regulates Sealing Zone Architecture and Dynamics in Cultured Osteoclasts. PLoS One. 2011; 6
66. Geblinger D, Geiger B, Addadi L. Surface-Induced Regulation of Podosome Organization Dynamics in Cultured Osteoclasts. Chembiochem. 2009; 10:158–65. [PubMed: 19065685]
67. Nakamura I, Takahashi N, Jimi E, Udagawa N, Suda T. Regulation of osteoclast function. Modern Rheumatology. 2012; 22:167–77. [PubMed: 21953286]
68. Fuller K, Ross JL, Szewczyk KA, Moss R, Chambers TJ. Bone Is Not Essential for Osteoclast Activation. PLoS One. 2010; 5
69. Geblinger D, Zink C, Spencer ND, Addadi L, Geiger B. Effects of surface microtopography on the assembly of the osteoclast resorption apparatus. J R Soc Interface. 2012; 9:1599–608. [PubMed: 22090285]
70. Chen J, Singh K, Mukherjee BB, Sodek J. Developmental expression of osteopontin (OPN) mRNA in rat tissues: evidence for a role for osteopontin in bone formation and resorption. Matrix. 1993; 13:113–23. [PubMed: 8492741]
71. Huq NL, Cross KJ, Ung M, Reynolds EC. A review of protein structure and gene organisation for proteins associated with mineralised tissue and calcium phosphate stabilisation encoded on human chromosome 4. Archives of Oral Biology. 2005; 50:599–609. [PubMed: 15892946]
72. Hunter GK, O'Young J, Grohe B, Karttunen M, Goldberg HA. The Flexible Polyelectrolyte Hypothesis of Protein-Biomineral Interaction. Langmuir. 2010; 26:18639–46. [PubMed: 20527831]
73. Hoang QQ, Sicheri F, Howard AJ, Yang DSC. Bone recognition mechanism of porcine osteocalcin from crystal structure. Nature. 2003; 425:977–80. [PubMed: 14586470]
74. Wang Y, Azais T, Robin M, Vallee A, Catania C, Legriel P, et al. The predominant role of collagen in the nucleation, growth, structure and orientation of bone apatite. Nature Materials. 2012; 11:724–33.
75. McKee MD, Nanci A. Ultrastructural, Cytochemical and Immunocytochemical Studies on Bone and Its Interfaces. Cells and Materials. 1993; 3(3):219–43.
76. Nanci A, Zalzal S, Gotoh Y, McKee MD. Ultrastructural characterization and immunolocalization of osteopontin in rat calvarial osteoblast primary cultures. Microsc Res Tech. 1996; 33:214–31. [PubMed: 8845520]
77. Beck GR, Zerler B, Moran E. Phosphate is a specific signal for induction of osteopontin gene expression. Proceedings of the National Academy of Sciences. 2000; 97:8352–7.
78. Rittling SR, Matsumoto HN, Mckee MD, Nanci A, An XR, Novick KE, et al. Mice Lacking Osteopontin Show Normal Development and Bone Structure but Display Altered Osteoclast Formation In Vitro. Journal of Bone and Mineral Research. 1998; 13:7.
79. Boskey AL, Spevak L, Paschalis E, Doty SB, McKee MD. Osteopontin deficiency increases mineral content and mineral crystallinity in mouse bone. Calcified Tissue International. 2002; 71:145–54. [PubMed: 12073157]
80. Shapses SA, Cifuentes M, Spevak L, Chowdhury H, Brittingham J, Boskey AL, et al. Osteopontin facilitates bone resorption, decreasing bone mineral crystallinity and content during calcium deficiency. Calcif Tissue Int. 2003; 73(1):86–92. [PubMed: 14506959]

81. Franzén A, Hultenby K, Reinholt FP, Önnerfjord P, Heinegård D. Altered osteoclast development and function in osteopontin deficient mice. Journal of Orthopaedic Research. 2008; 26:721–8. [PubMed: 18050311]
82. Huang WB, Carlsen B, Rudkin G, Berry M, Ishida K, Yamaguchi DT, et al. Osteopontin is a negative regulator of proliferation and differentiation in MC3T3-E1 pre-osteoblastic cells. Bone. 2004; 34:799–808. [PubMed: 15121011]
83. Sun J, Yin GY, Liu N. Effects of osteopontin from bovine milk on osteoblasts and osteoclasts co-culture system in vitro. Milchwiss-Milk Sci Int. 2011; 66:416–9.
84. Jang JH, Kim JH. Improved cellular response of osteoblast cells using recombinant human osteopontin protein produced by Escherichia coli. Biotechnol Lett. 2005; 27:1767–70. [PubMed: 16314968]
85. Jun IK, Jang JH, Kim HW, Kim HE. Recombinant osteopontin fragment coating on hydroxyapatite for enhanced osteoblast-like cell responses. J Mater Sci. 2005; 40:2891–5.
86. Kojima H, Uede T, Uemura T. In vitro and in vivo effects of the overexpression of osteopontin on osteoblast differentiation using a recombinant adenoviral vector. J Biochem. 2004; 136:377–86. [PubMed: 15598896]
87. Sun J, Liu N. Effects of osteopontin from bovine milk on osteoblasts in rat. Acta Nutrimenta Sinica. 2009; 31:356–60.
88. Arai N, Ohya K, Kasugai S, Shimokawa H, Ohida S, Ogura H, et al. Expression of bone sialoprotein mRNA during bone formation and resorption induced by colchicine in rat tibial bone marrow cavity. Journal of Bone and Mineral Research. 1995; 10:1209–17. [PubMed: 8585425]
89. Canfield AE, Farrington C, Dziobon MD, Boot-Handford RP, Heagerty AM, Kumar SN, et al. The involvement of matrix glycoproteins in vascular calcification and fibrosis: an immunohistochemical study. J Pathol. 2002; 196(2):228–34. [PubMed: 11793375]
90. Speer MY, McKee MD, Guldberg RE, Liaw L, Yang HY, Tung E, et al. Inactivation of the osteopontin gene enhances vascular calcification of matrix Gla protein-deficient mice: Evidence for osteopontin as an inducible inhibitor of vascular calcification in vivo. J Exp Med. 2002; 196:1047–55. [PubMed: 12391016]
91. McKee MD, Nanci A, Khan SR. Ultrastructural immunodetection of osteopontin and osteocalcin as major matrix components of renal calculi. Journal of Bone and Mineral Research. 1995; 10:1913–29. [PubMed: 8619372]
92. Thurgood LA, Wang T, Chataway TK, Ryall RL. Comparison of the Specific Incorporation of Intracrystalline Proteins into Urinary Calcium Oxalate Monohydrate Dihydrate Crystals. Journal of Proteome Research. 2010; 9:4745–57. [PubMed: 20672853]
93. Hirose M, Tozawa K, Okada A, Hamamoto S, Higashibata Y, Gao B, et al. Role of osteopontin in early phase of renal crystal formation: immunohistochemical and microstructural comparisons with osteopontin knock-out mice. Urological Research. 2012; 40:121–9. [PubMed: 21833789]
94. Evan AP, Coe FL, Rittling SR, Bledsoe SM, Shao YZ, Lingeman JE, et al. Apatite plaque particles in inner medulla of kidneys of calcium oxalate stone formers: Osteopontin localization. Kidney International. 2005; 68:145–54. [PubMed: 15954903]
95. Mo L, Liaw L, Evan AP, Sommer AJ, Lieske JC, Wu XR. Renal calcinosis and stone formation in mice lacking osteopontin, Tamm-Horsfall protein, or both. American Journal of Physiology-Renal Physiology. 2007; 293:F1935–F43. [PubMed: 17898038]
96. Amos FF, Dai L, Kumar R, Khan SR, Gower LB. Mechanism of formation of concentrically laminated spherules: implication to Randall's plaque and stone formation. Urological Research. 2009; 37(1):11–7. [PubMed: 19066874]
97. Amos, FF.; Olszta, MJ.; Khan, SR.; Gower, LB. Relevance of a Polymer-Induced Liquid-Precursor (PILP) Mineralization Process to Normal and Pathological Biomineralization. In: Königsberger, E.; Königsberger, L., editors. Biomineralization- Medical Aspects of Solubility. West Sussex, England: John Wiley & Sons, Ltd.; p. 2006p. 125-217.
98. Gower LB, Amos FF, Khan SR. Mineralogical Signatures of Stone Formation Mechanisms. Urological Research. 2010; 38(4):281–92. [PubMed: 20625894]

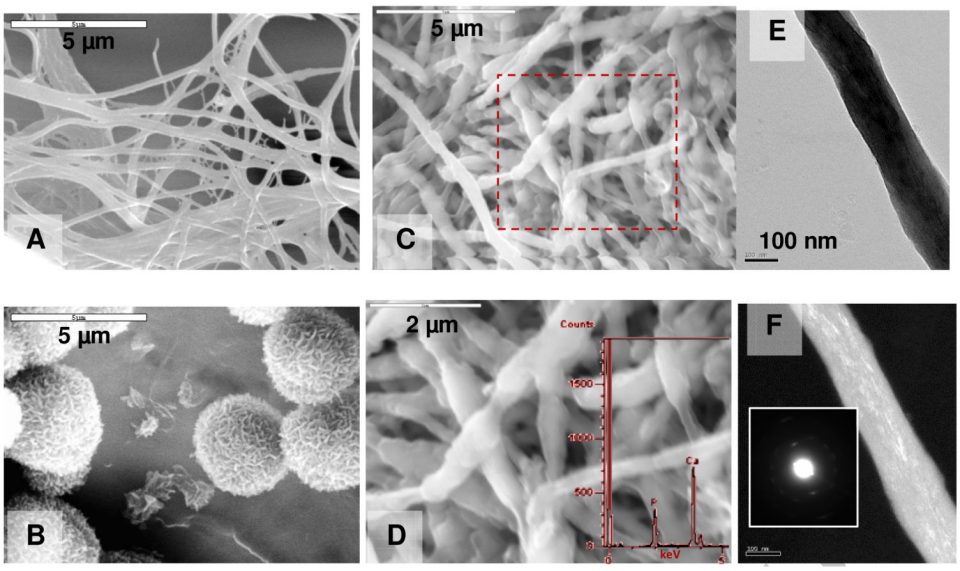

Figure 1.

Comparison of collagen sponge substrates mineralized without and with the PILP process. (A) SEM of the collagen sponge prior to mineralization. (B) SEM of the collagen sponge mineralized by the conventional crystallization process (without polymer additive). (C) SEM showing a collagen sponge treated with a PILP solution containing 200 μg/ml OPN as the process-directing agent. (D) A closer look and EDS analysis (inset) of the PILP-mineralized collagen fibrils from the area denoted by the dotted square on (C). (E) Bright- and (F) dark-field TEM micrographs of isolated collagen fibrils from a PILP-mineralized collagen sponge using OPN as process-directing agent. The (002) arcs were used to create the dark-field image, thus showing [001] aligned crystals, which appear as the bright streaks in the fibril. Scale bars denote 0.2 μm. (F) Inset: SAED pattern of the mineralized fibril, showing that the alignment of the hydroxyapatite nanocrystals are parallel to the collagen fibril.

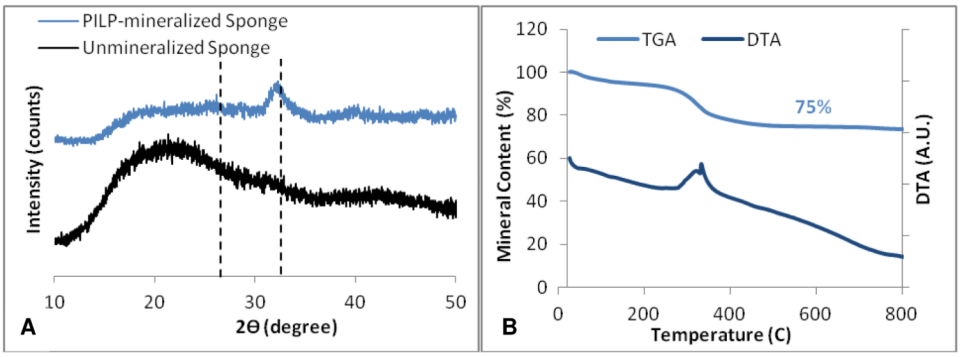

Figure 2.

Diffraction and thermal analysis of the PILP-mineralized collagen sponge using OPN as process-directing agent. (A) Wide-angle X-ray diffraction compares the sponge before and after mineralization. The peaks present at 26 and 32 degrees are indicative of hydroxyapatite. (B) An overlay of thermogravimetric analysis (TGA-top curve) and differential thermal analysis (DTA-bottom curve). TGA provides the overall mineral content of the sponge after the organic matter has been combusted, which yields 75 wt % mineral. The DTA curve of PILP-mineralized collagen sponge samples shows a low temperature peak at about 330°C, indicative of intrafibrillar mineral.

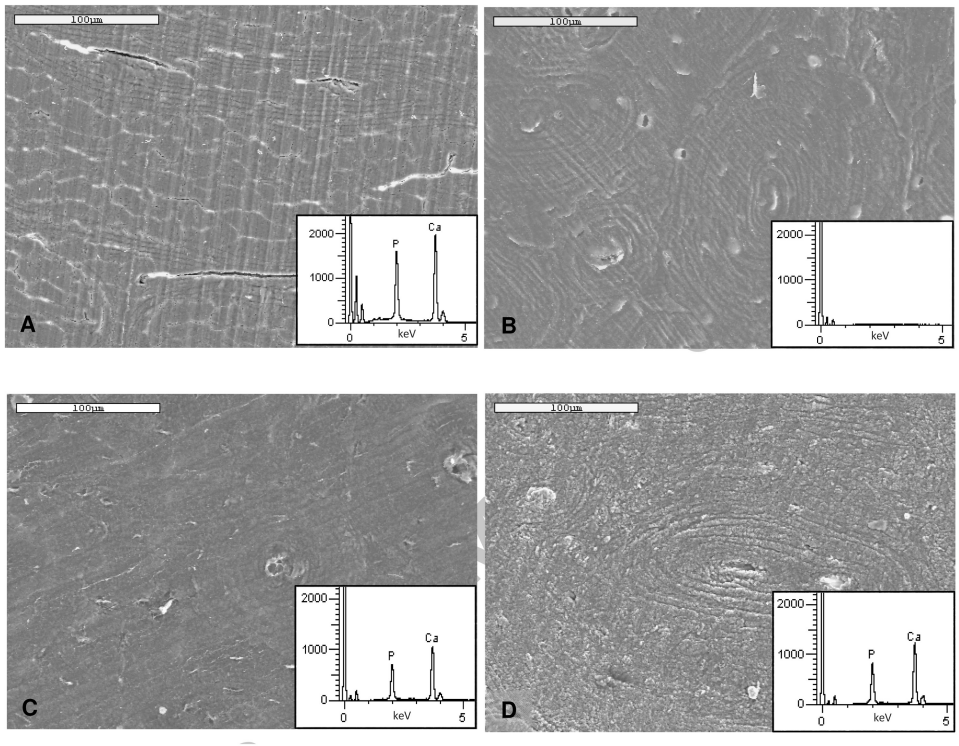

Figure 3.

SEM image of a native bovine bone specimen (A), of demineralized bone (B), and PILP remineralized specimens using polyaspartic acid (C), and PILP remineralized specimens using osteopontin as the process-directing agent (D). Representative EDS spectra for each group are also shown with the respective SEM micrographs, showing the lack of calcium and phosphorous in the demineralized specimens (B), and showing the presence of calcium and phosphorous in the remineralized specimens (C, D). The striations and cracks are knife marks and artifacts from sample preparation. Scale bar = 100 μm on all images.

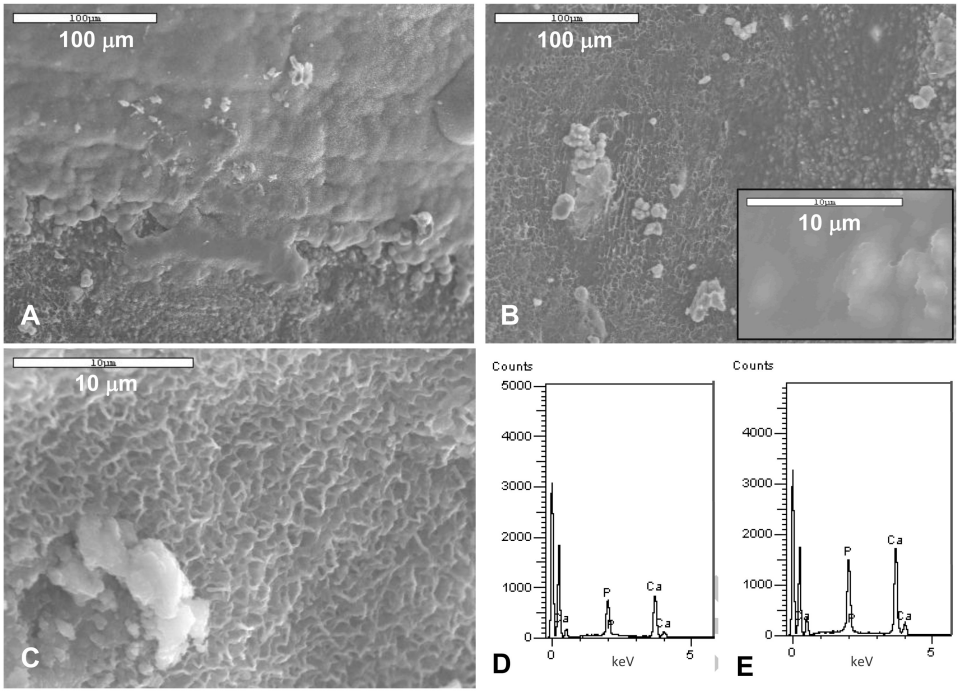

Figure 4.

Demineralized bone slice that was remineralized via the conventional crystallization process (without pASP additive). (A) Low magnification SEM image illustrating heterogeneity of the mineralized surface, where most of the surface was covered with a dense film of hydroxyapatite, interdispersed with regions lacking this coating. (B) A region without the coating shows a few scattered clusters of HA. The inset is a close up of the region that did not contain the coating which shows whitish clusters that appear to be below the surface of the collagen (C) A high magnification image of the mineral coating shows that the crystals are large and platy, typical of crystals grown via the conventional crystallization process. (D) EDS spectrum of a magnified region where there is no dense surface coating (inset of panel B) still shows the presence of mineral, attributed to the sub-surface mineral. (E) EDS of the regions of dense mineral films seen in the majority of the sample have large calcium and phosphorous peaks, as expected.

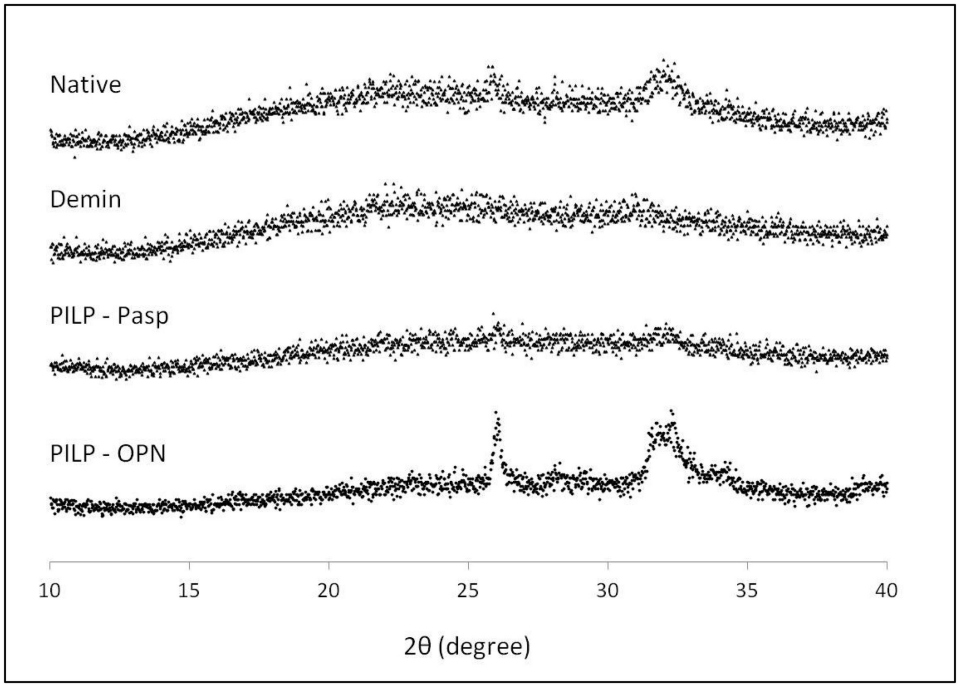

Figure 5.
WAXD patterns of native bovine bone, demineralized bone, and PILP remineralized bone specimens using either polyaspartic acid or osteopontin. The peaks present at 26 and 32 degrees are indicative of hydroxyapatite, and are broad due to the small crystallite size, as in bone

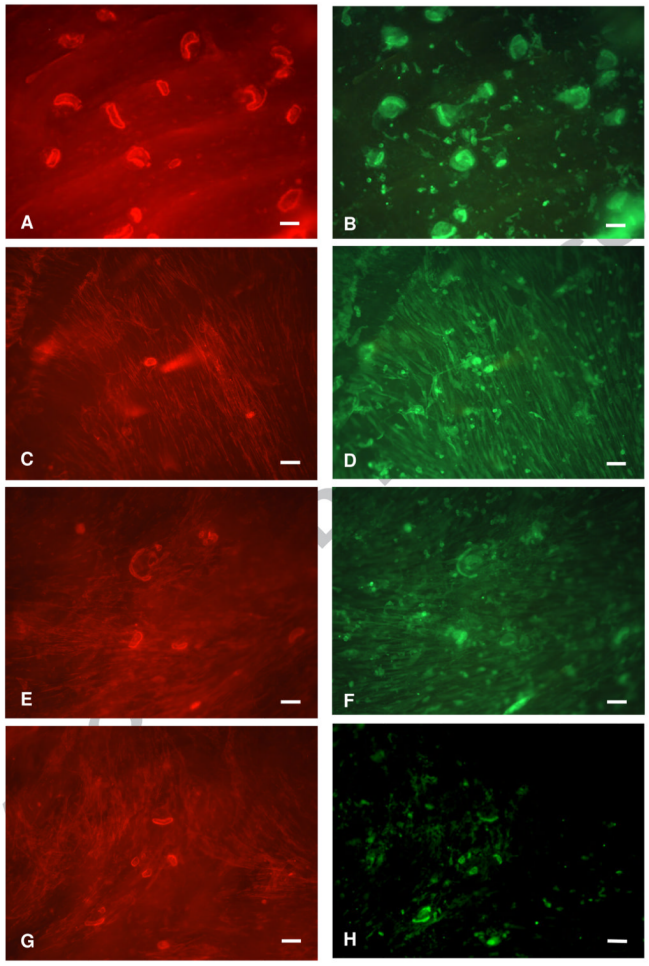

Figure 6.
Representative images of specimens stained with Texas red-tagged phalloidin to detect actin rings (Left: A, C, E, G), and with V-ATPase to detect ruffled borders (Right: B, D, F, H). (A, B) The native bone control shows the presence of both actin rings and ruffled membranes. (C, D) Demineralized bone shows some small actin rings, but there are very few, and there is a lot of stress actin. (E, F) The conventionally remineralized specimens show a few actin rings as well as the presence of stress actin from other cells. (G, H) PILP remineralized (with pASP process-directing agent) specimens show the presence of actin rings and ruffled membranes. The rings are smaller than in the bone control. Scale bars = 20 μm.

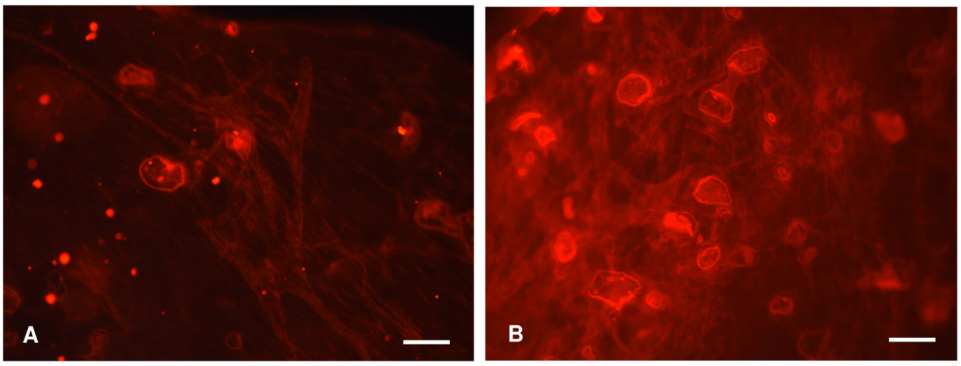

Figure 7.
Representative images of native bone (A) and PILP-remineralized bone with OPN process-directing agent (B). Specimens were stained with Texas red-tagged phalloidin to show the presence of actin rings which form the sealing zone. Scale bars = 20 μm.

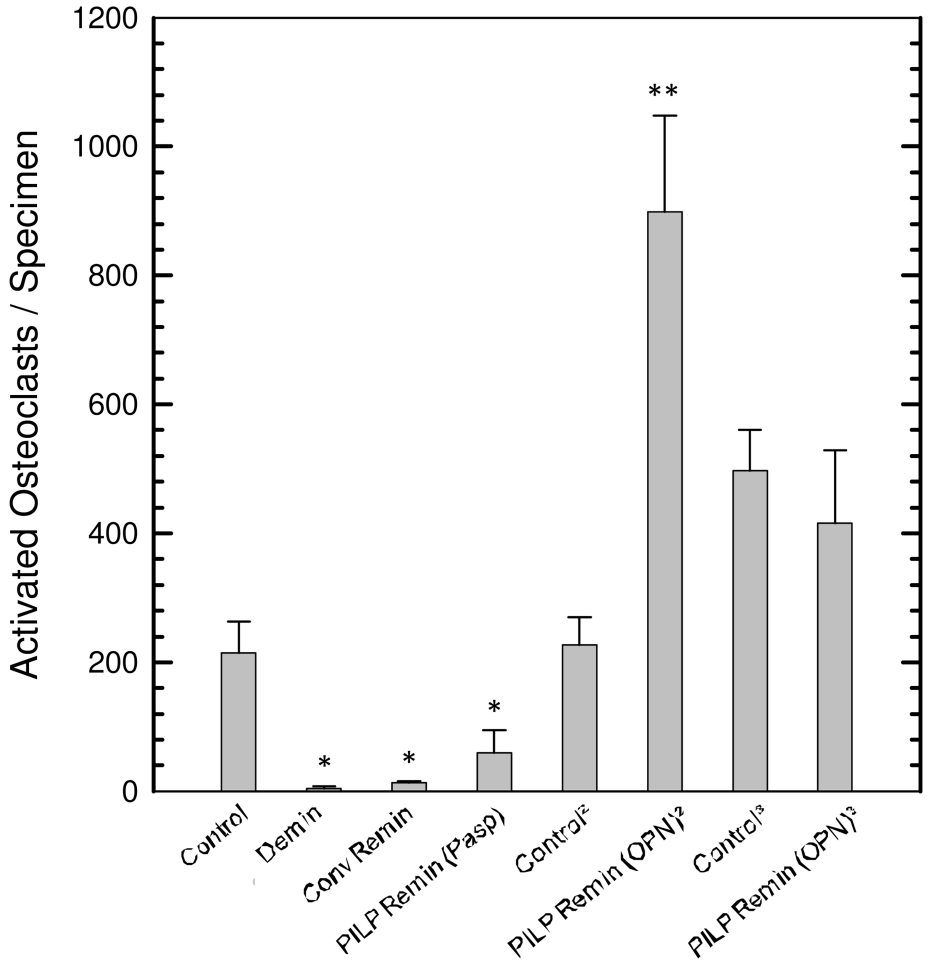

Figure 8.

Comparison of activated osteoclasts for each group tested, as measured by the average number of actin rings identified (error bars represent standard deviation). The groups labeled $(OPN)^2$ and $(OPN)^3$ are specimens tested in a second and third independent cell culture, where cells were harvested from different sets of mice for each study, and each with its own native bone sample as a control. All groups have an n=3, with the exception of $Control^2$ and $(OPN)^2$ with an n=4. *: $P<0.01$, **: $P<0.001$ relative to the respective native bone controls, assessed by unpaired t-test assuming unequal variance.

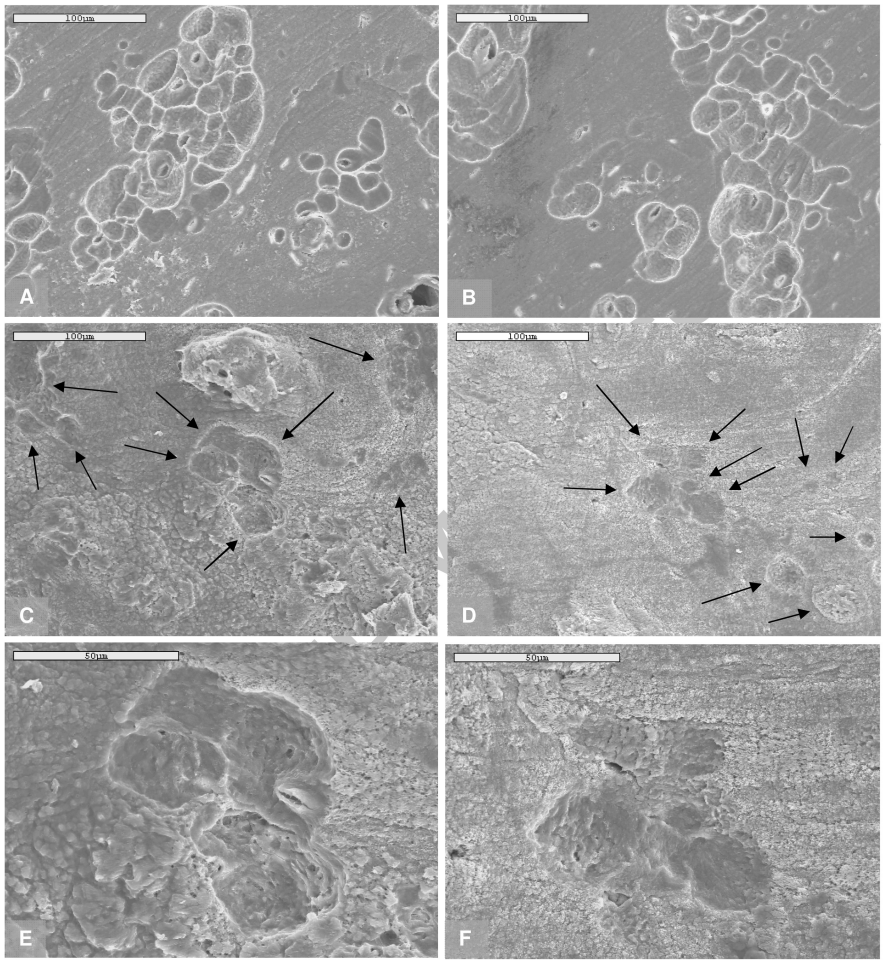

Figure 9.

SEM micrographs of post-culture surfaces of the positive control of native bone (A, B) and OPN PILP-remineralized specimens (C-F). Resorption pits are clearly seen in (A) and (B) and are also identified by arrows in (C) and (D). (E) and (F) are magnified images of (C) and (D), respectively. Scale bars = 100 μm in A – D, and 50 μm in E & F.